

Using Cellular Automata for porous media simulation

Olga Bandman

Received: DD MM. 2009 / Accepted: DD MM 2009

Abstract A cellular automata (CA) approach is proposed for simulating a fluid flow through the porous material with tortuous channels at pore level. The approach aims to combine CA methods both for constructing computer representation of porous material morphology and for simulating fluid flow through it. Porous medium morphology is obtained using CA whose evolution results in a stable configuration which is used as a porous medium morphological pattern for Lattice Gas CA application to simulate fluid flow through it and compute its permeability properties. Special boundary conditions are introduced allowing for different smoothness of solid pore walls surface. The model has been tested on a small 2D fragment in a PC and then implemented to investigate a porous carbon electrode of a hydrogen fuel cell on 128 processors of a multiprocessor cluster.

Keywords: cellular automata, Lattice-Gas models, pattern formation, porous medium, parallel implementation

1 Introduction

Fluid flow in porous materials is of great interest being extensively used both in engineering and research. A bright example of porous materials application is a hydrogen Proton Exchange Membrane Fuel Cell, the main parts of which – the polymer membrane and the carbon electrodes are made of porous substances, power generating capability of the cell strongly depending of the materials properties [1]. Obviously, simulation of processes in porous components is useful, and, sometimes, urgently needed both when the material is produced, and when the device is designed.

The problem of porous material simulation is not a new one. The earlier investigations are dated to the middle of the past century. At that time a porous medium

RAS Presidium Fundamental Research Program N 2, 2009(Project 6), SBRAS Integration Project 32-2009

Supercomputer Software Department
ICM&MG, Siberian Branch, Russian Academy of Sciences
Pr. Lavrentieva, 6, Novosibirsk, 630090, Russia
E-mail: bandman@ssd.sccc.ru

was regarded as a bulk substance, characterized by permeability and porosity. So, all calculations were based on the famous Darcy law connecting these two parameters. At the age of computer and numerical methods a number of mathematical models based on Partial Differential Equations were developed [2], being capable to simulate the fluid flow *at pore level*, i.e., simulating the flow through the pore channels. But, the capabilities of these models are limited for the following reasons. First, the construction of porous medium itself is a separate nontrivial problem. It is usually solved by representing porous medium morphology by randomly allocating simple geometrical figures like circles and rectangles of appropriate size. Such an approximation is sometimes too coarse, especially when soft porous materials such as polymers or carbons are under consideration. The second problem lays in the complexity of the differential equations solution. The flow is to be simulated by the nonlinear Navier-Stokes equation, which is a hard and sometimes impracticable task due to the complex boundary conditions and difficulty of parallel implementation. To make the problem easier convection-diffusion models [2] based on linear partial differential equations is frequently used. In both cases the irregularity of pores configuration makes the task stiff.

A seminal idea of “computing from images” has been proposed in [3]. It is intended to be used with fine grained simulation models, where the explicit form of computational process representation on a lattice allows to map it onto the pixels of the material image. The investigation presented in this paper is based on a similar approach, but implemented on CA level.

With the appearing of Lattice-Gas CA hydrodynamics [4] the investigations of porous materials at porous level (as a flow in pores) make progress rapidly, the majority of methods used being based on the Lattice-Boltzmann method (LBM) [6]. A short but complete review of LBM methods implementation for porous material study is given in [7]. Some of them are very sophisticated allowing for permeability prediction and calculating the tortuosity of the flow. Very impressive results are presented in [8,9], where 3D flows are simulated at pore level.

For all that, there remain many aspects to be studied. Some of them motivate the approach used in the paper. They are as follow.

- 1) Although Lattice-Boltzmann hydrodynamics is considered to be more advanced and is nowadays more frequently used, the classic form of Lattice Gas CA has its advantages. The first is the absence of round off errors, and the second is computational stability, both features being the consequence of the completely discrete representation of all values used in simulation process. A not the least of the factor is the desire to expand the CA simulation methods, combining CA hydrodynamics with CA pattern formation methods for porous medium investigation.

- 2) Cellular Automata techniques give an opportunity to obtain porous medium model by exploiting CA capability of pattern formation. The proper choice of CA parameters allows to obtain the pore model with given a priori characteristics. So, one of the objectives of the paper is to introduce and test the method of obtaining the medium model using CA techniques.

- 3) It is quite clear, that for simulating even a small specimen a very large cellular automaton is needed. Hence, parallel implementation is unavoidable, and its efficiency should also be taken into consideration when evaluating the method features. The fact that simulation is accomplished over a composition of two CA with identical size and data types, makes reasonable the parallelization of both cellular CA as a single task.

Based on these three arguments a CA approach to simulation of a fluid flow through porous medium is presented. The approach is constrained to static porous media, whose

morphology does not change when the liquid fills its pores. After the Introduction, in Section 2, the problem statement is given intuitively and formally. In section 3 the porous medium model and its computer representation are described. Section 4 is devoted to the boundary conditions. In section 5 the results of testing the method on a single computer and its parallel implementation on a supercomputer cluster are presented.

2 The Problem Statement

Simulation of fluid flow through a porous material aims to investigate the material properties. Simulation methods and computer tools are in demand when the material production is under development, and also when a certain device is designed where the flow through the porous membrane is used, or on the contrary, such a flow should be prevented.

Porous medium itself is a very complex entity for computer simulation. One of the reasons is that it cannot be found two porous material specimens which are quite identical. This fact imposes indeterminacy in porous media mathematical description. Hence, simulation methods can not claim to have a high degree of accuracy. Most likely, the simulation results should be regarded as qualitative ones, although some quantitative characteristics can also be obtained.

The simulation method here is developed for the 2D case with assumption to be an approximation of the 3D one, the latter being of actual interest. In our approach an attempt is made to develop fluid flow simulation process together with the procedure of obtaining the porous medium morphology model. Thus, the whole simulation model turns out to be a superposition $\aleph = \aleph_F(\aleph_P)$ [10] of two cellular automata: $\aleph_P = \langle A_P, M, \Theta_P \rangle$ and $\aleph_F = \langle A_F, M, \Theta_F \rangle$, where \aleph_P and \aleph_F stand for porous medium morphology and for flow model, respectively. The first may be either synchronous or asynchronous pattern formation CA, the second is synchronous Lattice-Gas CA. Both of them have identical naming sets $M_P = M_F = M = \{(i, j) : i, j = 0, \dots, N\}$, but different alphabets $A_P \neq A_F$ and different transition function sets $\Theta_P \neq \Theta_F$. The composed model allows us to perform a number of simulations with changed initial conditions for \aleph_P in order to obtain properties of several specimens slightly differing in patterns but having the same morphology type (motif) inherent to porous material under investigation. Performing a number of simulations on those patterns with the same motif one may obtain far more reliable information about the porous properties.

The simulation task is formulated as follows. Given are two sets of parameters: 1) concerning porous material, and 2) concerning the flowing liquid.

The first is characterized by the following data.

- 1) The *size* of the specimen $X \times Y$.
- 2) *Porosity* coefficient

$$Por = S_0/S_1, \quad (1)$$

where S_0 and S_1 are the areas occupied by pores and solids, respectively, on a specimen $X \times Y$ in size.

3) *Resistance* of porous medium to the flow. The notion is newly introduced here. If the main stream is along the x -axis then

$$Res = L_x/L_y, \quad (2)$$

where L_x is the length of the projection of the total pore-solid border onto the x -axis, and L_y – onto the y -axis, calculated for the area $X \times Y$ in size.

4) *Tortuosity*. Although the notion is qualitative we introduce a quantitative assessment, which is expressed through the amounts of extremities in the pore border function $y(x)$, i.e.

$$Tor = |T_{extr}|,$$

where

$$T_{extr} = \{(x, y) : (dx/dy = 0 \ \& \ d^2x/dx^2 \neq 0) \vee (dy/dx = 0 \ \& \ d^2y/dy^2 \neq 0)\}. \quad (3)$$

5) *Smoothness of pore walls*. This property characterizes the interfacial tension between the liquid and solid. It has a quantitative measure as a *wetting angle*, which depends on the solid and liquid substances properties and for most porous materials it cannot be assessed. Hence, we confine ourselves to qualitative estimate in terms of *smooth* and *rough*.

6) Morphological type which characterizes pore channel configurations. Following [11], we classify them according to the associations with common life pictures (patches, stripes, clouds, islands) which are referred to as *motifs*.

The second set of given data includes the liquid substance properties: density and viscosity, as well as the initial condition: the pressure drop or the mean velocity. Usually, the fluid is assumed to inflow from one side (say, the left one) of the specimen and to outflow on the opposite side. Transition to CA parameters from the given physical values and back after simulation is done according to [15].

Each program simulation run aims to produce the following information.

1) The flow rate Q , i.e. the amount of liquid passing through the specimen in a unit of time .

2) The flow velocity distribution $V(i, j)$ in pores (velocity field, maximum velocity, existence of vortices, cavities).

A series of simulation runs allows to obtain some useful dependencies of Q and $V(i, j)$ on pressure drop, channel tortuosity, porosity and smoothness of pore walls.

3 CA Models of Porous Media

CA that may be successfully used to construct porous medium morphology belong to class 2 of the Wolfram's classification [12]. The class comprises CA exhibiting self-organization, i.e. their evolution tends to a stable global state. Configurations obtained during the evolution look like fancy patterns resembling the morphology of porous medium, where black areas formed by cells in state $v(i, j) = 1$ correspond to solid substance, and white areas formed by cells with $v(i, j) = 0$ represent the empty space of pores. Properties of patterns in the evolution may be regulated by changing the CA parameters and the initial configuration.

Two types of pattern formation CA are the most suitable for being used for porous medium model construction. They are as follows.

1) The class of so called "phase separation CA" [13].

2) The CA with weighted templates, which are more known as Cellular Neural Networks (CNN) [11].

To represent $\aleph_P = \langle A, M, \theta \rangle$ formally, it is enough to specify its *alphabet* $A = \{0, 1\}$, the set of cell coordinates $M = \{(i, j) : i = 0, \dots, I; j = 0, \dots, J\}$ in a *cellular array*

$\Omega = \{(v, (i, j)) : A \in A; i = 0, \dots, I; j = 0, \dots, J\}$, where a pair $(v, (i, j))$ is referred to as a *cell* [14].

A set of neighboring cells nearest to $(v, (i, j))$ is defined as a *local configuration* $S(i, j)$

$$S(i, j) = \{(v_0, (i, j)), \dots, (v_k, \phi_k(i, j)), \dots, (v_q, \phi_q(i, j))\}, \quad (4)$$

where $V_S = \{v_0, v_1, \dots, v_q\}$ is a *state template* of $S(i, j)$, and

$$T_S = \{(i, j), \phi_1(i, j), \dots, \phi_k(i, j), \dots, \phi_q(i, j)\} \quad (5)$$

is the *spacial template* for $S(i, j)$. The functions $\phi_k(i, j)$, defined on M , indicate the coordinates of cells that form a *neighborhood* for a cell (i, j) .

Functioning of the CA is given by a *local operator*, which consists of two local configurations with a substitution symbol in between.

$$\theta(i, j) : S(i, j) \rightarrow S'(i, j), \quad (6)$$

where $S(i, j)$ and $S'(i, j)$ are referred to as a *basic*, and a *next state* local configurations, respectively, $V_{S'} = \{v'_0, \dots, v'_r\}$, $r \leq q$, being a *next-state template* of $S'(i, j)$ and (i, j) — a *main cell* for θ . Next states $v'_k \in V_{S'}$, $k = 0, \dots, r$, are values of a *transition function*

$$v'_k = f_k(v_0, \dots, v_q), \quad k = 0, 1, \dots, r. \quad (7)$$

In \aleph_P the transition functions are either Boolean functions or simple arithmetical ones. Application of θ to a cell $(i, j) \in M$ consists of two actions:

- 1) computing next states according to (7), and
- 2) updating cells of $S(i, j)$ assigning the obtained values to the corresponding cell states.

Application of $\theta(i, j)$ to all $(i, j) \in M$ transforms a cellular array $\Omega(t)$ into $\Omega(t+1)$. The sequence

$$\Sigma(\Omega) = \Omega(0), \Omega(1), \dots, \Omega(t), \Omega(t+1), \dots, \Omega(\hat{t}) \quad (8)$$

is called *the evolution*, t being the iteration number, and $\Omega(0)$ - the initial cellular array. During the evolution the cellular array changes its black-white pattern tending to a stable global configuration.

Each CA produces a scope of patterns characterized by similar features, which define a certain motif. There is no strict method for CA synthesis by the given properties of the resulting pattern. Moreover, in the range of patterns produced by one and the same CA, a great variety of patterns, differing in tortuosity, porosity and orientation of black-white borders may be obtained by variation of initial cellular array. Also, when running the iterative process of evolution it is possible to observe the sequence of produced patterns and stop the process at any moment when $\Omega(t)$ meets the wanted parameters.

Example 1 CA $\aleph_P = \langle A, M, \theta \rangle$ is a model of the process of phase-separation. Being applied to a cellular array $\Omega(0)$ with randomly distributed “ones” and “zeroes”, this CA gradually aggregates the “ones” in patches of fancy forms. The parameters of \aleph_P are as follows. $A = \{0, 1\}$, the CA size is $I \times J = 300 \times 300$,

$$\theta : \{(v_{kl}, (i - k, j - l)) : k, l = -r, \dots, r\} \rightarrow (v', (i, j)), \quad (9)$$

where

$$v' = \begin{cases} 1, & \text{if } s = (q-1)/2 \text{ or } s > (q+1)/2, \\ 0, & \text{if } s = (q+1)/2 \text{ or } s < (q-1)/2, \end{cases} \quad (10)$$

where

$$q = (2r+1)^2, \quad s = \sum_{kl=0}^q v_{kl}$$

In Fig.1 three patterns produced by \aleph_P are shown. The simulation was performed with periodic boundary conditions. The initial cellular array is a random distribution of “ones” in $\Omega(0)$ with average density $\rho = 0.5$. From the resulting evolution of \aleph_P the properties of porous media represented by the obtained pattern, are easily computed according to (1-3). Thus, the patterns in Fig.1 are characterized by the porosity $Por \simeq 0.6$. The tortuosity of the pattern at $t = 10$ is 10 times larger than that at $t = 50$. As for the resistance, it is equal for both patterns, being approximately $Res \simeq 0.55$.

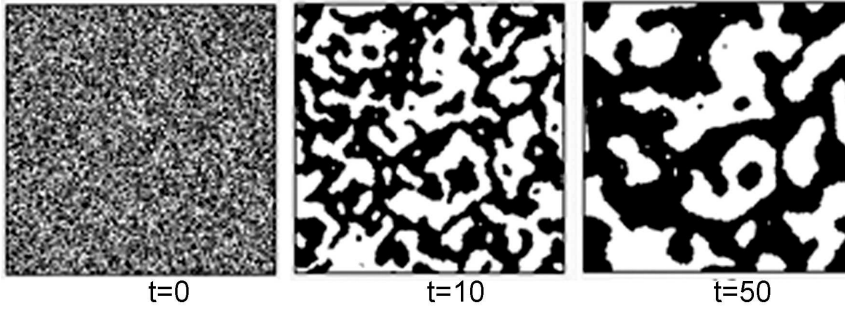


Fig. 1 Three snapshots obtained while simulating the evolution of a CA \aleph_P , given by (9,10)

Example 2 Two CA $\aleph_P = \langle A, M, \theta \rangle$, and $\aleph_{P'} = \langle A, M, \theta \rangle$, which differ in mode of operation and in initial cellular arrays produce the patterns with different motifs.

Both CA have Boolean alphabets, are equal in size $I \times J = 400 \times 400$ and the following local operator.

$$\theta : \{(v_0, (i, j)), (v_{-r, -r}, \phi_{-r, -r}(i, j)), \dots, (v_{r, r}, \phi_{r, r}(i, j))\} \rightarrow (v'_0, (i, j)), \quad (11)$$

where $r = 3$, $q = (2r+1)^2$.

$$\begin{aligned} \phi_{g,h}(i, j) &= (i+g, j+h), \quad g, h = -r, -r+1, \dots, -1, 0, 1, \dots, r+1; \\ v'_0 &= \begin{cases} 1, & \text{if } \sum_{g=-r}^r \sum_{h=-r}^r w_{g,h} v(i+g, j+h) > 0 \\ 0, & \text{otherwise,} \end{cases} \end{aligned} \quad (12)$$

where

$$w_{g,h} = \begin{cases} 1, & \text{if } |g| \leq 1 \ \& \ |h| \leq 1 \\ -0, 2 & \text{otherwise.} \end{cases}$$

The first CA (\aleph_P) operates in synchronous mode. Being applied to a cellular array $\Omega(0)$ having randomly distributed “ones” with density $\rho = 0.001$, it produces “round

spots " of equal size randomly located over the array (Fig.2a). In the process of the evolution the spots grow in diameter, exhibiting the decrease of the porosity coefficient of the corresponding cellular array. When the porosity match the wanted value the evolution stops. The second CA

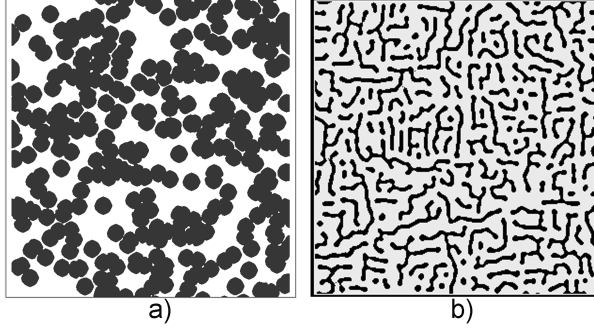


Fig. 2 Two patterns obtained by evolution of two CAs with weighted templates, and θ_2 , given by (11,12): a) with synchronous mode of operation and initial density $\rho = 0,001$, b) with asynchronous mode of operation and initial density distributions $\rho_i = 0.008$.

$\aleph_{P'}$ operates in asynchronous mode, starting with an initial cellular array $\Omega(0)$ having randomly distributed "ones" and "zeroes " with the density $\rho_i = 0.008$. The obtained pattern is inverted turning the formatted black stripes into solids and leaving the the white area for pores (Fig.2b).

4 CA-Model of the Flow

The CA for fluid flow simulating $\aleph_F = \langle A_F, M_F, \Theta \rangle$, is a Gas-Lattice FHP CA-model [4,5] with special boundary conditions. The flow is represented by abstract particles, moving and colliding in a discrete hexagonal space. The naming set is given by the set of hexagons coordinates $M = \{(i, j) : i = 0, 1, \dots, I; j = 0, 1, \dots, J\}$.

The distances between two neighboring cells are assumed to be equal to 1. The naming template contains six nearest neighboring cells, i.e.

$$T(i, j) = \{(i, j), \phi_1(i, j), \dots, \phi_6(i, j)\}, \quad (13)$$

Each cell may have up to 6 particles, each being provided with a velocity directed towards one of the neighbors. The cell state alphabet contains Boolean vectors 6 bit long: $A = \{(v_1, \dots, v_k, \dots, v_6) : v_k \in \{0, 1\}, |A| = 2^6\}$. A component $v_k = 1$ of a state vector indicates that the cell $(\mathbf{v}, (i, j))$, has a particle moving towards the k th neighbor with a velocity $v_k = 1$. Particle mass is equal to 1.

The cellular array Ω consists of four parts: Ω_P , Ω_W , Ω_{In} , and Ω_{Out} , containing pore cells, wall cells, input cells and output cells, respectively.

The CA functioning is determined by global superposition [10] of two local operators $\Theta = \theta_1(\theta_2)$, where θ_1 represents particles propagation, being identical for all cell types, and θ_2 simulates the collision, its transition functions being different for different cell types.

$$\theta_1(i, j) : \{(\mathbf{v}_0, (i, j)) \dots, (\mathbf{v}_1, \phi_1(i, j)), \dots, (\mathbf{v}_6, \phi_6(i, j))\} \rightarrow \{(\mathbf{v}', (i, j))\}, \quad (14)$$

where

$$\mathbf{v}'(i, j) = \bigvee_{l=0}^6 v_l(\phi_{l+3}(i, j)). \quad (15)$$

Here and further summation of indices is $+\text{mod}6$. For pore cells in Ω_P

$$\theta_2(i, j) : \{(\mathbf{v}_0, (i, j))\} \rightarrow \{(\mathbf{v}_0', (i, j))\}. \quad (16)$$

The transition function in (16) $\mathbf{v}_0' = f(\mathbf{v}_0)$ is, usually, given in the form of a table, some arguments having equiprobable outcomes. All transition rules (16) satisfy the laws of mass and momentum conservation. The mode of operation is synchronous.

In cells from Ω_W the transition functions $f(\mathbf{v}_0)$ depend on the smoothness, tortuosity and irregularities of solid pore wall surface. So, it is impractical to search a general expression for boundary condition. When Lattice-Gas models are used for simulation flows in tubes or other reservoirs with wall lines, two types of boundary conditions are used: *no-slip* (bounce-back) conditions for rough wall surface and *slip* conditions (based on specular rules) for smooth surface. Unfortunately, the latter may not be used for tortuous pore walls without violating the law of mass conservation. Hence, the reasonable decision is to use *bounce-back* rules in all cases, regulating the smoothness of walls by means of changing the type of some cells in the subset $\Omega_B \in \Omega$, referred to as *border layer*,

$$\Omega_B = \{(i, j) : (i, j) \in \Omega_W \ \& \ T(i, j) \bigcap \Omega_P \neq \emptyset\} \quad (17)$$

The bounce-back collision rule θ_{b-b} prescribes the particle entering the wall cell to reverse its direction.

$$\theta_{b-b} : (\mathbf{v}, (i, j)) \rightarrow (\mathbf{v}', (i, j)) \quad \forall (i, j) \in B, \quad (18)$$

where the components of $\mathbf{v}'(i, j)$ are

$$v'_k = v_{k+3} \quad (19)$$

The bounce-back rules do not conserve moments, which is in correspondence with energy dissipation due to friction between liquid and solid. Bounce-back rules are appropriate to weak roughness, when the fluid velocity is zero in the nearest vicinity of the wall.

When pore materials under investigation have very rough walls, the following technique is applied. A certain number of cells $(i, j) \in \Omega_P$ such that

$$|T(i, j) \bigcap \Omega_W| = 2 \quad (20)$$

are transferred from Ω_P to Ω_W to form some additional obstacles to the flow. Similarly, if the porous material under investigation has a very smooth pore walls, some cells $(i, j) \in \Omega_B$, satisfying

$$|T(i, j) \bigcap \Omega_P| = 4 \quad (21)$$

should be transferred to Ω_P , resulting in removing the protrusions of solid walls. In both cases the cell $(i, j) \in \Omega_B$ to be transformed from one type to the other are chosen with probability p_B . The effect of surface property change is the strongest when $p_B = 0.5$.

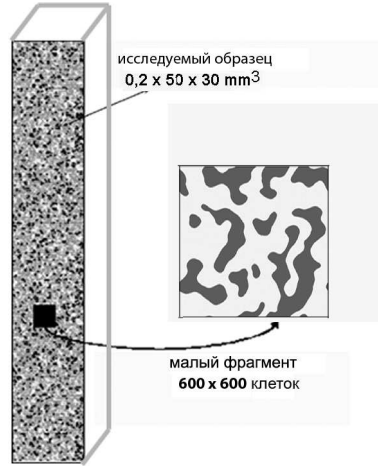


Fig. 3 A porous carbon cathode and its small prototype fragment, used for the computational test experiments

5 Implementation of the Method

The proposed approach is implemented for simulating the flow of water through a carbon cathode in Proton Exchange Fuel Cell [1]. In this device the electrodes and the membrane are made of porous materials, therefore its performance depends on their properties. Application of the method to a real size specimen requires parallel implementation on many processors. So, beforehand, in order to prove out the proposed method in more details, it was tested on a small prototype fragment (Fig.3)

Parameters of the CA-model are determined according to the method of mapping physics onto CA-models [15] as follows.

1. Porous cathode has the size $0.2 \times 50 \times 30 \text{ mm}^3$. The mean diameter of pore channel is $10 \text{ m}\mu\text{m}$. According to the theory and practice of porous medium [2] simulation, the smallest channel should be more than 10 times wider than the model length unit, so, the length scale is chosen to be $Sc(l) = h = 0.2 \text{ m}\mu\text{m}$, which yields the 2D model size of the given specimen to be 1000×250000 cells.

2. Since the CA viscosity of FHP-I [5] is proved to be $\nu_{CA} = 0.85^1$ and the viscosity of water is $\nu_w = 10^{-4} \text{ m}^2 \text{ s}^{-1}$, the viscosity scaling coefficient is $Sc(\nu) = 1.17 \cdot 10^{-5} \text{ m}^2 \text{ s}^{-1}$.

3. The obtained two scales: $S(l)$ and $Sc(\nu)$ allow to calculate all other relations between the given physical values and their CA counterparts. They are as follows:

- particle mass $m_p = \rho_w / (h^3 \times 6) = 2.7 \cdot 10^{-18} \text{ kg}$,
- time scale $Sc(t) = \tau = h^2 / Sc(\nu) = 3.5 \cdot 10^{-8} \text{ s}$,
- velocity scale $Sc(v) = Sc(l) / Sc(t) = 0.57 \cdot 10^{-3} \text{ ms}^{-1}$,

The most important characteristic of a porous material under investigation is a value of the flux $Q \text{ kgs}^{-1}$, i.e. the amount of liquid passing through the specimen in a time unit. It has a physical meaning only for a 3D case. In 2D approximation the specimen is assumed to be homogeneous along the third direction. Based of such an

¹ 0.85 is a value obtained after Galilean invariance correction for the mean CA density $\rho \approx 0.3$

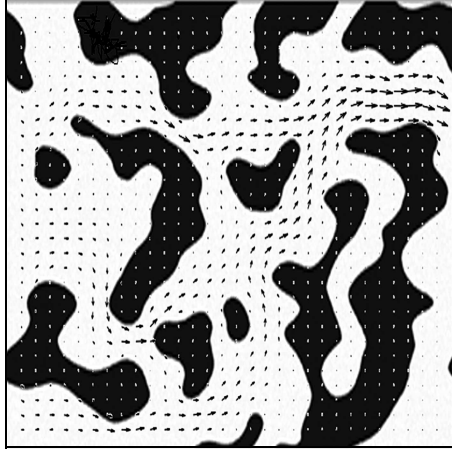


Fig. 4 The velocity field obtained after 4000 iterations while simulating the fluid flow through the prototype fragment.

assumption the following formula is used to calculate Q .

$$Q = \frac{F \cdot K \cdot m_p}{\tau} \text{ kgs}^{-1}, \quad (22)$$

where F is a number of particles passing through the 2D CA during an iteration, computed during the simulation, and K is the CA size along the third direction.

For testing the proposed method on a personal computer and to observe the process in its dynamics a prototype fragment of the size 600×600 cells has been chosen, which is 700 times smaller than the real size. The porous medium morphology has been constructed using a “phase separation CA” (Example 1). The initial global configuration $\Omega(0)$ has been obtained by randomly distributing “ones” and “zeroes” with the mean density 0.5. The proper tortuosity has been chosen while observing the evolution of \aleph_P .

The simulation has been performed for three different degrees of pore walls smoothness, obtained by transferring certain border cells from Ω_W to Ω_P with probabilities $p_B = 0.2$ and $p_B = 0.4$. The results of the fragment simulation in CA-model values are given in Table 1.

Table 1 CA-simulation results : F — number of particles passing through the test fragment per iteration, $\langle v \rangle$ — mean velocity at $t = 4000$ for three different pore walls surfaces

property	p_B	Q	$\langle v \rangle$
weak rough	0	36.5	0.85
smooth	0.2	40.9	0.87
very smooth	0.4	42.1	0.88

For investigating the real size specimen ($0.2 \times 50 \times 30 \text{ mm}^3$) the simulation has been performed on 150 Dual Core processors Intel Xeon of the Cluster K-100 in Joint Supercomputer Center of Russian Academy of Sciences using MPI library. The cellular array was decomposed into 150 domains each being of size 1000×1000 . The porous

specimen with weak wall roughness ($p_w = 0$) has been investigated. The total time of simulation is $T_p + T_F = 284$ s with $T_p = 7, 8$ s, T_P, T_F being the evolution times of \aleph_P and \aleph_F , respectively. The model flow F through the specimen with $K=150000$ and porosity $\text{Por}=0,608$ is 83867 particles/iteration, which makes $Q = 182.92 \text{ gs}^{-1}$ through a 3D specimen of 30 mm wide.

6 Conclusion

A method for determining properties of porous material using CA-models is presented. The method is based on the composition of two CA: the first constructs a computer representation of porous medium morphology, the second simulates the fluid flow through it. The method is given in 2D approximation, although its extension onto a 3D case is associated only with 2^6 times increase of computational complexity. That is just the increase of alphabet cardinality when transiting to a 3D model RD-1 [16]. Moreover, the interactiveness of the method allows to the researcher to construct a porous medium morphology, to modify it and to obtain the needed data using one and the same program. Of course there remain many open problems. In theoretical aspect the main problem is the creation of formal methods of CA synthesis by a given set of patterns generated by its evolution. The most urgent practical problem is to determine qualitative characteristics of porous morphology properties for the most used classes of porous materials.

References

1. Larminie J, Dicks A. (2003) Fuel Cells Systems Explained. John Willey & Sons, N.-Y.
2. Sahimi M(1993) Flow phenomena in rocks: from continuum models to fractals, percolation, cellular automata and simulated annealing. Rev in Modern Phys 65(4): 1393–1533.
3. Edward J, Garboczi E, Bentz DP, Snyder KA, Martys NS, Stutzman PE, Ferraris CF, and Jeffrey W. Modelling and Measuring the Structure and Properties of Cement-based Materials. An electronic monograph. Nat Inst of Standards and Technology (<http://ciks.cbt.nist.gov/gar-boczi/>).
4. Rothman BH, Zaleski S. (1997) Lattice-Gas Cellular Automata. Simple Models of Complex Hydrodynamics. Cambridge Univ. Press, London.
5. Frish U, d’Humières D, Hasslacher B, Lallemand P, Pomeau Y, Rivet JP (1987) Lattice-Gas hydrodynamics in two and three dimensions. Complex Systems, 1: 649–707.
6. Succi S (2001) The Lattice Boltzmann Equation for Fluid Dynamics and Beyond. Oxford University Press, NY.
7. Nabovati A, Sousa ACM (2007) Fluid Flow Simulation In Random Porous Media At Pore Level Using The Lattice Boltzmann Method. J of Eng Sci and Techn 2, No 3: 226–237.
8. Clague DS, Kandhai D, Zang R, Slood PMA (2000) Hydraulic permeability of (un)bounded fibrous media using the Lattice Boltzmann method. Phys Rev E, 61(1): 616–625.
9. Pan C, Hilpert M, Miller CT (2001) Pore-scale modeling of saturated permeabilities in random sphere packings. Phys Rev E, 64(6), Art N 006702.
10. Bandman O (2005) Composing Fine-Grained Parallel Algorithms for Spatial dynamics Simulation. In: Malyskin V(ed) LNCS 3606. Springer, Berlin: 99–113.
11. Chua L (2002) CNN: a Paradigm for Complexity. World Scientific, Singapore.
12. Wolfram S (1984) Universality and complexity in cellular automata. Physica D, 10: 1-35.
13. Toffoli T, Margolus N (1987) Cellular Automata Machines. MIT Press, USA.
14. Achasova S, Bandman O, Markova V, Piskunov S (1994) Parallel Substitution Algorithm. Theory and Application. World Scientific, Singapore.
15. Bandman O (2008) Mapping physical phenomena onto CA-models. In AUTOMATA-2008. Theory and Application of Cellular Automata. Adamatsky A, Alonso-Sanz R, Lawiczak A, Martinez GJ, Morita K, Worsch Th. (eds). Luniver Press, UK: 391-397.
16. Medvedev YuG (2003) Three dimensional Cellular Automata Model of Viscous Fluid Flow. Avtometriya 39, 3: 43–50 (in Russian)